



Chemical modification of pro-inflammatory proteins by peroxynitrite increases activation of TLR4 and NF- κ B: Implications for the health effects of air pollution and oxidative stress

Kira Ziegler^{a,1}, Anna T. Kunert^{a,1}, Kathrin Reinmuth-Selzle^a, Anna Lena Leifke^a, Dariusz Widera^b, Michael G. Weller^c, Detlef Schuppan^{d,e}, Janine Fröhlich-Nowoisky^a, Kurt Lucas^{a,**}, Ulrich Pöschl^{a,*}

^a Max Planck Institute for Chemistry, Multiphase Chemistry Department, 55128, Mainz, Germany

^b Stem Cell Biology and Regenerative Medicine Group, School of Pharmacy, University of Reading, RG6 6AP, Reading, UK

^c Federal Institute for Materials Research and Testing (BAM), Berlin, Germany

^d Institute of Translational Immunology, University Medical Center of the Johannes Gutenberg University, 55131, Mainz, Germany

^e Division of Gastroenterology, Beth Israel Deaconess Medical Center, Harvard Medical School, MA, 02215, USA

ARTICLE INFO

Keywords:

Protein modification
TLR4
Peroxynitrite
 α -Synuclein
HSP60
HMGB1

ABSTRACT

Environmental pollutants like fine particulate matter can cause adverse health effects through oxidative stress and inflammation. Reactive oxygen and nitrogen species (ROS/RNS) such as peroxynitrite can chemically modify proteins, but the effects of such modifications on the immune system and human health are not well understood. In the course of inflammatory processes, the Toll-like receptor 4 (TLR4) can sense damage-associated molecular patterns (DAMPs). Here, we investigate how the TLR4 response and pro-inflammatory potential of the proteinous DAMPs α -Synuclein (α -Syn), heat shock protein 60 (HSP60), and high-mobility-group box 1 protein (HMGB1), which are relevant in neurodegenerative and cardiovascular diseases, changes upon chemical modification with peroxynitrite.

For the peroxynitrite-modified proteins, we found a strongly enhanced activation of TLR4 and the pro-inflammatory transcription factor NF- κ B in stable reporter cell lines as well as increased mRNA expression and secretion of the pro-inflammatory cytokines TNF- α , IL-1 β , and IL-8 in human monocytes (THP-1). This enhanced activation of innate immunity via TLR4 is mediated by covalent chemical modifications of the studied DAMPs.

Our results show that proteinous DAMPs modified by peroxynitrite more potently amplify inflammation via TLR4 activation than the native DAMPs, and provide first evidence that such modifications can directly enhance innate immune responses via a defined receptor. These findings suggest that environmental pollutants and related ROS/RNS may play a role in promoting acute and chronic inflammatory disorders by structurally modifying the body's own DAMPs. This may have important consequences for chronic neurodegenerative, cardiovascular or gastrointestinal diseases that are prevalent in modern societies, and calls for action, to improve air quality and climate in the Anthropocene.

1. Introduction

Reactive oxygen and nitrogen species (ROS/RNS) like peroxynitrite play important roles in oxidative stress and adverse health effects induced upon exposure to environmental pollutants and in the course of inflammatory diseases [1–4]. Peroxynitrite (ONO₂⁻) is generated upon reaction of superoxide (O₂⁻) and nitric oxide (NO) [5]. It can react with

amino acids like tyrosine, leading to the formation of nitrotyrosine, dityrosine, and protein oligomers [6–8]. Nitrotyrosine and dityrosine are known as markers of inflammation and oxidative stress, which can influence the chemical and physiological properties of proteins [9–11]. For example, nitration can change the binding of proteins to certain receptors and thus modulate downstream signaling cascades [7,12,13]. Notably, preferential recognition of nitrotyrosine epitopes by

* Corresponding author.

** Corresponding author.

E-mail addresses: k.lucas@mpic.de (K. Lucas), u.poeschl@mpic.de (U. Pöschl).

¹ equal co-author contributions.

Abbreviations

α -Syn	α -Synuclein
HSP60	heat shock protein 60
HMGB1	high-mobility-group box 1 protein
OVA	ovalbumin
TLR4	Toll-like receptor 4
NF- κ B	nuclear factor 'kappa-light-chain-enhancer' of activated B-cells
DAMP	damage-associated molecular patterns
IL	interleukin

immunoglobulins was reported for several inflammatory diseases [14–16]. Dityrosine crosslinks can be intra- or intermolecular, altering protein structures, causing protein aggregation/oligomerization, and affecting protein function [17,18].

During inflammation, damage-associated molecular patterns (DAMPs) can be actively secreted by epithelial cells, monocytes, macrophages, and other cells, or passively released by damaged and dying cells [19]. Proteinous DAMPs can have various intracellular functions, e.g., as chaperones, and when released as extracellular proteins, they can stimulate pattern recognition receptors (PRR) such as the Toll-like receptor 4 (TLR4) [20]. TLR4 signaling leads to the activation of transcription factors like the nuclear factor 'kappa-light-chain-enhancer' of activated B-cells (NF- κ B) and the interferon regulatory transcription factor 3 (IRF3), which are key activators of inflammatory cascades [21]. NF- κ B induces the expression and modulates the secretion of pro-inflammatory cytokines such as TNF- α , IL-1 β , and IL-8, which can stimulate the corresponding cytokine receptors leading to further activation of NF- κ B and other signaling pathways [22–25]. This positive feedback can amplify and propagate inflammatory processes in autocrine or paracrine fashion [26,27].

In this study, we investigate if and how peroxynitrite can enhance the activation of TLR4 and NF- κ B by chemical modification of disease-related proteins acting as DAMPs (Table S1): α -Synuclein, heat shock protein 60, and high-mobility-group box 1 protein.

α -Synuclein (α -Syn) is a neuronal protein that regulates exocytosis and endocytosis of synaptic vesicles as well as ATP synthase [28–30]. Oxidative and nitrating conditions can lead to the formation of nitrated, misfolded or aggregated α -Syn, which is linked to neurodegenerative disorders such as Parkinson's disease [31]. Oligomeric and misfolded α -Syn can be released from neuronal cells by exocytosis and stimulate TLR4 and other receptors [32,33].

Heat shock protein 60 (HSP60) is a mitochondrial chaperone that assists correct folding of imported mitochondrial proteins [34]. HSP60 can be released by stressed or necrotic cells, and modulate immune response by stimulating TLR4 and other receptors [35,36]. It contributes to the pathogenesis of chronic inflammatory diseases such as Crohn's disease, diabetes, and atherosclerosis [37].

High-mobility-group box 1 protein (HMGB1) is a ubiquitously expressed nuclear protein involved in DNA replication, recombination, transcription, and repair [38]. HMGB1 can be released by activated or damaged cells and secreted by immune cells in response to microbial or pro-inflammatory stimuli [39]. HMGB1 can stimulate TLR4, the advanced glycosylation end product-specific receptor (RAGE), and other receptors [19]. It is involved in severe acute and chronic diseases, such as sepsis, cancer, cardiovascular and neurodegenerative diseases [40–42].

The investigated proteins were exposed to peroxynitrite, and covalent chemical modifications were analyzed by liquid chromatography (HPLC), gel electrophoresis (SDS-PAGE), and western blots (anti-nitrotyrosine, anti-dityrosine). TLR4 and NF- κ B activation were determined in stable reporter cell lines with bioluminescence detection. The HeLa TLR4 dual luciferase reporter cell line was used for specific

detection of TLR4 activation and simultaneous determination of cell viability. The THP-1-Lucia™ NF- κ B cell line was used to detect NF- κ B activation via TLR4 or other receptors such as TLR2 and RAGE. Human monocytes (THP-1) were used to investigate mRNA expression and secretion of inflammation-related cytokines, such as TNF- α , IL-1 β , and IL-8.

2. Materials and methods

2.1. Protein modification and analysis

2.1.1. Peroxynitrite modification

Protein stock solutions (1 mg mL⁻¹) of α -Syn (Merck Millipore, Darmstadt, Germany), HSP60 (Abcam, Cambridge, UK), HMGB1 (Sigma Aldrich, Taufkirchen, Germany), and Ovalbumin (InvivoGen, Toulouse, France) were prepared in PBS (Thermo Fisher Scientific, Darmstadt, Germany). Ammonium bicarbonate ($\geq 98\%$, Ph. Eur., BP, Carl Roth, Karlsruhe, Germany) was dissolved in water to yield a final buffer concentration of 2 M, and the pH was adjusted to 7.8 by the addition of 1 M hydrogen chloride (37% stock solution, Merck Millipore). For each reaction, 300–500 μ L protein solution was transferred into a brown reaction tube (Eppendorf, Hamburg, Germany), and 7.5–12.5 μ L ammonium bicarbonate buffer (2 M) was added to yield a final buffer concentration of 50 mM. After being thawed on ice, 1–8 μ L sodium peroxynitrite solution (160–200 mM, Merck Millipore) was added to yield a molar ratio of peroxynitrite to tyrosine residues of 5:1, and the reaction was performed on ice for 110 min. Thereafter, the sample was pipetted into a 10 kDa centrifugal filter (Amicon®, Merck Millipore) and centrifuged at 14,000 $\times g$ for 2 min (5427 R, Eppendorf). The sample was washed five times with 200 μ L PBS and centrifugation at 14,000 $\times g$ for 2 min. For sample recovery, the filter was turned upside down, transferred into a clean microcentrifuge tube, and centrifuged at 1000 $\times g$ for 2 min. To recover possible sample residues, the filter was washed with 200 μ L fresh PBS and centrifuged upside down at 1000 $\times g$ for 2 min into the concentrated protein sample. Ovalbumin (OVA), which is not a TLR4 agonist, was treated the same way and served as negative control in the cell culture experiments described below. For mock samples, 500 μ L pure PBS was mixed with 12.5 μ L ammonium bicarbonate buffer (2 M) and 8 μ L peroxynitrite and treated as described above.

Protein concentrations were determined using a Synergy Neo plate reader (BioTek, Bad Friedrichshall, Germany) measuring the absorbance at 260 nm/280 nm. For each protein, a dilution series of the native protein (25–1000 μ g mL⁻¹) was used for calibration. Three microliters of modified protein solution were transferred into a micro-volume plate in triplicates (Take3 trio, BioTek), and the absorbance was measured. The protein concentrations were confirmed by SDS-PAGE and silver stain (see section 2.1.3).

For each of the investigated proteins, multiple samples of protein solution were chemically modified as outlined above, and selected samples were characterized by the analytical methods described below. An overview of the analytical results is given in Table S2 (tyrosine nitration degree, dimer fraction).

2.1.2. HPLC-DAD analysis

For the investigated proteins, tyrosine nitration degrees were determined as described in Selzle et al. [43]. Briefly, an HPLC–DAD system (Agilent Technologies 1260 Infinity series, Waldbronn, Germany) equipped with a monomerically bound C₁₈ column (Vydac 238 TP, 250 mm \times 2.1 mm i.d., 5 μ m, Hichrom, Berkshire, UK) was used for chromatographic separation. Gradient elution was performed with 0.1% (v/v) trifluoroacetic acid in water (VWR International GmbH, Darmstadt, Germany) and acetonitrile (Carl Roth), and absorbance was measured at wavelengths of 280 nm and 357 nm. Injection volume was 10 μ L, and each chromatographic run was performed in duplicates. For system control and data analysis, ChemStation Software

was used (Rev. C.01.07, Agilent). Nitration was observed in the modified samples of all proteins, and tyrosine nitration degrees were quantified in two independent experiments as specified in Table S2. The tyrosine nitration degree is defined as the concentration of nitrotyrosine divided by the sum of the concentrations of nitrotyrosine and tyrosine [43].

2.1.3. SDS-PAGE and silver stain

Protein oligomerization was visualized and quantified by silver stained SDS-PAGE (Thermo Fisher Scientific). Protein samples dissolved in PBS were mixed with an equivalent volume of 2x Laemmli buffer, containing 65.8 mM Tris-HCl (pH 6.8, Carl Roth), 26.3% glycerol (v/v, Carl Roth), 2.1% SDS (Carl Roth), 0.02% bromophenol blue (Sigma Aldrich) and 5.0% 2-mercaptoethanol (Sigma Aldrich), and heated at 95 °C for 5 min. The samples (50 ng in 10 µL) were loaded onto PROTEAN Precast gels (4–20%, Bio-Rad, Munich, Germany) together with 10 ng Color Prestained Protein Standard, Broad Range (11–245 kDa, New-England Biolabs, Frankfurt, Germany) and stained with a silver stain kit (Thermo Fisher Scientific) following manufacturer's instructions. For image acquisition and quantification of protein monomers, dimers, and higher oligomers, a ChemiDoc system (Bio-Rad) with Image Lab software 5.2.1 (Bio-Rad) was used. Protein dimers occurred in the modified samples of all proteins (Fig. S1, Table S2), and signals of higher oligomers were observed but exceeded the analytical detection limit (3%) only for modified HSP60 (23 ± 13%).

2.1.4. Western blot analysis

The presence of nitrotyrosine and dityrosine residues was investigated by SDS-PAGE and subsequent Western blot analysis. The native and modified protein samples were prepared in Laemmli-buffer as described in section 2.1.3. As sensitivities for the antibodies varied, different amounts of protein per lane were applied for nitrotyrosine staining (2 µg α-Syn, 5 µg HSP60, and 10 µg HMGB1) and dityrosine staining (5 µg α-Syn, 5 µg HSP60, and 5 µg HMGB1). For nitrotyrosine staining, α-Syn, HSP60, and HMGB1 were separated by a 12%, 8%, and 10% SDS polyacrylamide gel, respectively, and by a Mini-PROTEAN Precast gel (4–20%, Bio-Rad) for dityrosine staining. Thereafter, the gels were transferred onto 0.45 µm PVDF membranes (Merck Millipore) using a semi-dry transfer unit (Hoefer, Holliston, MA, USA). The membranes were blocked with 5% fat-free milk powder (Cell Signaling Technology, Leiden, Netherlands) in Tris-buffered saline with 0.1% Tween-20 (TBS-T) at RT for 2 h, followed by an overnight incubation at 4 °C with nitrotyrosine antibody (mouse monoclonal [clone HM11], 1:1000, Cat # 321,900, Thermo Fisher Scientific) and dityrosine antibody (mouse monoclonal [clone 7D4], 1:10,000, Cat # NBP2-59360, Novus Biologicals, Centennial, CO, USA), respectively, diluted in 5% fat-free milk powder in TBS-T. All membranes were washed four times with TBS-T for 5 min each and incubated with the horseradish peroxidase coupled secondary antibody (goat anti-mouse, polyclonal, 1:10,000, Cat # 115-035-062, Jackson Immuno Research Europe Ltd, Ely, UK) at RT for 1 h, diluted in TBS-T. For detection, the membranes were washed four times with TBS-T for 5 min, and protein bands were developed using the chemiluminescence system ECL-femto (Thermo Fisher Scientific) for nitrotyrosine and ECL-plus (Thermo Fisher Scientific) for dityrosine according to the manufacturer's protocol. The bands were detected in a ChemiDoc system, and images were processed using Image Lab software 5.2.1. Nitrotyrosine and dityrosine were detected in peroxynitrite-modified samples of all investigated proteins. For the native proteins, neither nitrotyrosine nor dityrosine were detectable in the western blots (Fig. S1).

2.1.5. Endotoxin quantification

The amount of endotoxin in native and modified protein samples was quantified by a Pierce™ LAL Chromogenic Endotoxin Quantitation Kit (Thermo Fisher Scientific) according to the manufacturer's protocol. For this purpose, protein stock solutions were diluted to 1 µg mL⁻¹ with

endotoxin-free water. The endotoxin level in all protein samples was less than 1 EU per µg of protein.

2.2. Cell culture experiments

All cell experiments were performed with the same final concentrations of native and modified protein samples (α-Syn: 50.0 µg mL⁻¹, HSP60: 14.3 µg mL⁻¹, HMGB1: 3.6 µg mL⁻¹, OVA: 50.0 µg mL⁻¹) except for mRNA expression of α-Syn (35.7 µg mL⁻¹). LPS from *E. coli* O111:B4, 25 ng mL⁻¹, InvivoGen) was used as positive control (LPS-EB for HeLa TLR4 experiments; LPS-EB ultrapure for THP-1-Lucia™ and THP-1 experiments), and medium and mock served as negative controls. Protein solutions were diluted in the respective cell culture medium.

2.2.1. HeLa TLR4 dual reporter cells

Using an immortalized and further modified HeLa TLR4 dual luciferase reporter cell line (Novus Biologicals), we simultaneously determined TLR4 activation and cell viability [8]. HeLa is a human epithelial cervix cell line, which is not known to express functional receptors of TLR4, TLR2 or RAGE. The stably transfected TLR4/MD-2/CD14/IL-8 Prom/LUCPorter™ reporter cell line expresses human TLR4 (Novus Biologicals). This cell line was further stably co-transfected with a Renilla luciferase reporter gene under the transcriptional control of an IL-8 promoter [8] serving as a surrogate marker for viability to investigate both TLR4 activation and cell viability simultaneously. Cells were grown in Dulbecco's Modified Eagle's Medium (DMEM, Thermo Fisher Scientific) containing 25 mM D-glucose and 1 mM sodium pyruvate supplemented with 10% heat-inactivated fetal bovine serum (FBS superior, Cat #S0615, Lot #0973F, Biochrom, Berlin, Germany), 1% penicillin/streptomycin (Thermo Fisher Scientific) and 140 µg mL⁻¹ hygromycin B (InvivoGen) in a humidified atmosphere of 5% CO₂ at 37 °C. For each sample and replicate, 20,000 HeLa TLR4 dual reporter cells in 100 µL medium per well were seeded in a flat-bottom 96-well plate (Greiner, Frickenhausen, Germany). After 24 h, the cells were incubated in triplicates with 50 µL of the respective protein or control sample for 7 h. Thereafter, cells were washed with 200 µL PBS and lysed using 15 µL passive lysis buffer (Promega, Mannheim, Germany) at -80 °C overnight. The read out was performed using the Dual-Luciferase® Reporter Assay System (Promega) according to the manufacturer's protocol. Both luminescence signals were measured in a Synergy Neo plate reader. To calculate the normalized TLR4 activity, TLR4-driven Renilla luciferase signal was divided by the constitutive, CMV-driven firefly luciferase signal that served as a surrogate marker for cell viability. For each experiment, LPS-treated cells were used as a positive control, and the arithmetic mean was set to 100%. This value was used to normalize the measurement results of all protein and control samples. Arithmetic mean values and standard deviations were calculated from the normalized values of three (HSP60) or four (α-Syn, HMGB1, OVA) independent experiments performed in triplicates.

2.2.2. THP-1 NF-κB reporter cells and receptor antagonists

THP-1-Lucia™ NF-κB (InvivoGen) is an immortalized modified THP-1 cell line allowing the determination of NF-κB activation by measuring the activity of secreted luciferase. We used this cell line to determine the activation of NF-κB after treatment with native and peroxynitrite-modified proteins, regardless of the receptors involved in the activation (TLR4, TLR2, RAGE). Cells were grown in Roswell Park Memorial Institute (RPMI) 1640 medium (Thermo Fisher Scientific) containing 25 mM D-glucose and 1 mM sodium pyruvate supplemented with 10% heat-inactivated FBS, 100 µg mL⁻¹ Zeocin™ (InvivoGen), and 1% penicillin/streptomycin in a humidified atmosphere of 5% CO₂ at 37 °C. For each sample and replicate, 100,000 cells in 50 µL medium per well were seeded in a flat-bottom 96-well plate. To inhibit TLR4 or RAGE signaling, cells were pre-incubated with 50 µL of the TLR4 antagonist TAK-242 or the RAGE antagonist FPS-ZM1 for 4 h. TAK-242 (25 mM, Merck

Millipore) was provided in dimethyl sulfoxide (DMSO) and further diluted with medium to a final concentration of $0.36 \mu\text{g mL}^{-1}$. FPS-ZM1 (25 mg, Merck Millipore) was dissolved in 250 μL DMSO and further diluted with medium to a final concentration of $3.3 \mu\text{g mL}^{-1}$. If no antagonist was applied, 50 μL medium was added to the cells. Subsequently, cells were incubated in triplicates with 50 μL of the respective protein or control samples for 24 h. Cells treated with DMSO in medium ($4.4 \mu\text{g mL}^{-1}$) showed no NF- κB activation or toxic effects. Activity of NF- κB was measured by QUANTI-Luc™ reagent (InvivoGen) according to manufacturer's instructions. Briefly, 10 μL of cell culture supernatant was transferred into a white plate (LUMITRAC™, Greiner), and mixed with 50 μL of QUANTI-Luc™ reagent. The luminescence was detected in a Synergy Neo plate reader. For each experiment, LPS-treated cells were used as positive control, and the arithmetic mean was set to 100%. This value was used to normalize the measurement results of all protein and control samples. Arithmetic mean values and standard deviation were calculated from the normalized values of three ($\alpha\text{-Syn}$) or four (HSP60, HMGB1, OVA) independent experiments performed in triplicates. Assessment of cell viability was performed in triplicates using the alamarBlue™ cell viability reagent (Thermo Fisher Scientific) according to the manufacturer's protocol. Excitation was performed at 560 nm, and emission was measured at 590 nm in a Synergy Neo plate reader.

2.2.3. Cytokine immunoassay

Immortalized human THP-1 monocyte cells (ATCC, Manassas, VA, USA) were used as typical monocytes producing inflammation-related cytokines such as TNF- α , IL-1 β , and IL-8. THP-1 monocytes express functional TLR4, TLR2, and RAGE, whose activation leads to NF- κB

activation and subsequent production and release of cytokines. Cells were grown in RPMI 1640 medium supplemented with 10% heat-inactivated FBS, 0.05 mM 2-mercaptoethanol (Sigma Aldrich), and 1% penicillin/streptomycin. Quantification of cytokine secretion was performed using a multiplex immunoassay. For each sample and replicate, 100,000 human THP-1 monocytes in 100 μL medium per well were seeded in a flat-bottom 96-well plate (Greiner) and incubated in triplicates with 50 μL of the respective protein or control samples over 24 h. Thereafter, cells were centrifuged at $200 \times g$ for 5 min (5427 R, Eppendorf), and the supernatants of the triplicates were combined and analyzed in duplicates for TNF- α , IL-1 β , and IL-8 by a multiplex assay kit (R&D systems Inc., Minneapolis, MN, USA) according to the manufacturer's protocol. The read-out was performed on a MAGPIX device (Luminex, Austin, TX, USA), and arithmetic mean values and standard deviation of the duplicates were calculated. Three experiments were performed (first two with same supernatant) and showed similar trends. Assessment of cell viability was performed as described in section 2.2.2.

2.2.4. mRNA extraction and qPCR analysis

Quantification of mRNA expression of TNF- α , IL-1 β , IL-8, and CXCL-10 was performed using real-time quantitative PCR (qPCR). For each sample, 400,000 human THP-1 monocyte cells in 1 mL medium per well were seeded in a 6-well cell culture plate (Greiner). On the next day, cells were incubated with 1 mL of the respective protein or control samples for 4 h. For qPCR analysis, cells were harvested by centrifugation at $500 \times g$ for 5 min. Total RNA was extracted from cells using RNeasy Mini Kit (Qiagen, Hilden, Germany) following the spin technology protocol. Total RNA yield was determined using a Take3 trio micro-volume plate in a Synergy Neo plate reader. Using the High

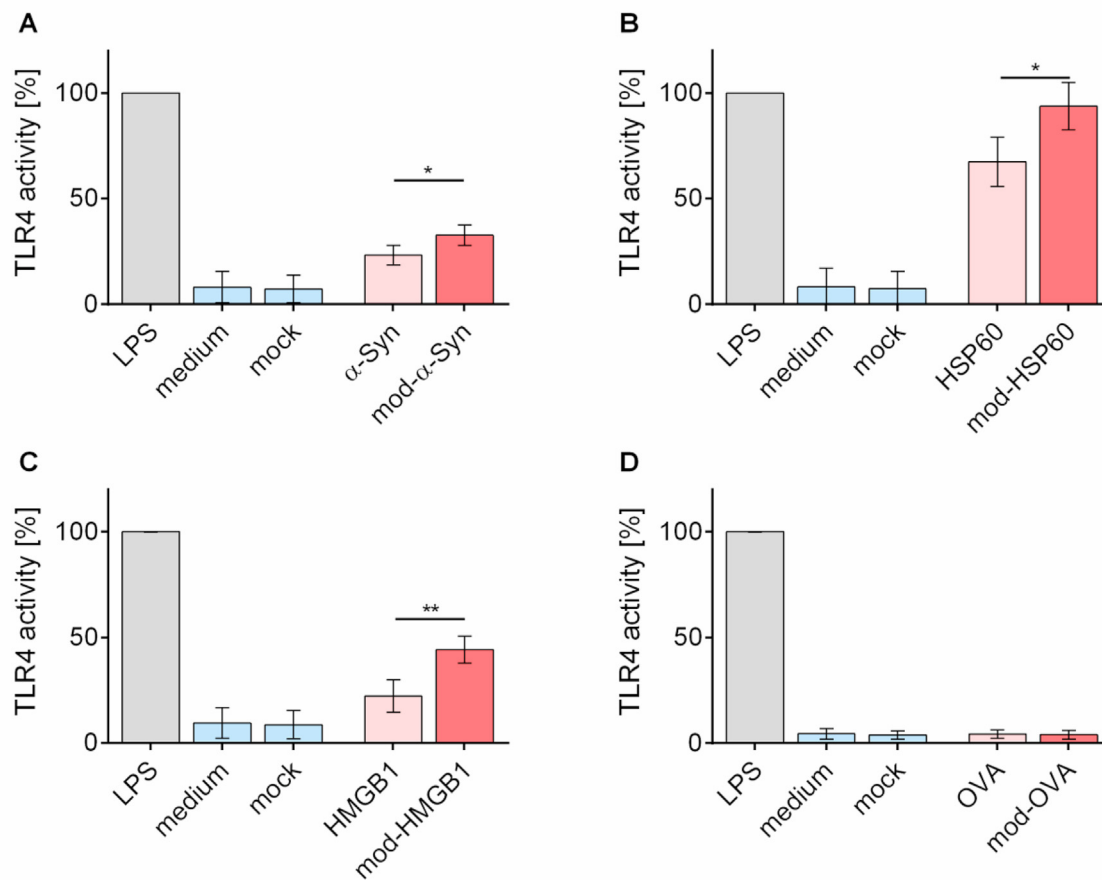


Fig. 1. TLR4 activation by native and peroxynitrite-modified proteins. TLR4 activity in HeLa TLR4 dual luciferase reporter cells determined for $\alpha\text{-Syn}$ (A), HSP60 (B), HMGB1 (C), and OVA (D) normalized to LPS. Arithmetic mean values and standard deviations of three to four independent experiments performed in triplicates (* $p < 0.05$, ** $p < 0.01$).

Capacity cDNA Reverse Transcription Kit (Thermo Fisher Scientific), 500 ng of total RNA per sample were transcribed into cDNA. Afterwards, qPCR was performed in duplicates using 10 ng of cDNA mixed with SsoAdvanced Universal SYBR Green Supermix (Bio-Rad) to a final concentration of 333 nM for each primer, which were designed using PrimerBlast (NCBI) and the respective template genes (Table S3). As reference genes served peptidylprolyl isomerase A (PPIA) and TATA-binding protein (TBP). Reactions were performed at 98 °C for 30 s, followed by 37 cycles of 98 °C for 10 s, and 60 °C for 25 s. Gene expression was calculated according to the $2^{-\Delta\Delta CT}$ method using the Bio-Rad CFX Manager Software 3.1. Arithmetic mean values and standard deviation of the duplicates were calculated. Three independent experiments were performed showing similar trends.

2.2.5. Statistical analyses

GraphPad Prism version 6.07 (GraphPad, San Diego, CA, USA) was used for statistical analysis. Unpaired t-tests were performed to observe differences between the native and peroxynitrite-modified proteins. The results were considered as significant when * $p < 0.05$, ** $p < 0.01$, *** $p < 0.005$.

3. Results

For the investigated proteins in native and peroxynitrite-modified form, TLR4 and NF- κ B activation were determined in stable reporter cell lines. The HeLa TLR4 dual luciferase reporter cell line was used for specific detection of TLR4 activation and simultaneous determination of cell viability, while the THP-1-Lucia™ NF- κ B cell line was used to detect NF- κ B activation. Additionally, mRNA expression and secretion of inflammation-related cytokines induced by NF- κ B were measured in human monocytes (THP-1).

As shown in Figs. 1 and 2, chemical modification by peroxynitrite significantly increased activation of TLR4 and NF- κ B for all three investigated proteins. Relative to the native protein, the TLR4 activity increased by a factor of ~1.4 for α -Syn and HSP60 and by a factor of ~2.2 for HMGB1 (Fig. 1, Table S4), while the NF- κ B activity increased by a factor of ~1.6 for α -Syn and HSP60 and by a factor of ~4.2 for HMGB1 (Fig. 2, Table S4). Inhibition of TLR4 by the antagonist TAK-

242 reduced the NF- κ B response to both, the modified and native protein, by more than 80% for α -Syn, by more than 90% for HSP60, and by 30–40% for HMGB1, while the RAGE inhibitor FPS-ZM1 had no substantial effect (Fig. 2). These inhibition experiments indicate that the enhancement of NF- κ B activation by peroxynitrite-modification is predominantly mediated by TLR4 for α -Syn and HSP60, while for HMGB1 also other receptors such as RAGE and TLR2 may be involved [44,45].

Fig. 3 shows that the chemically modified proteins also enhanced the secretion of the pro-inflammatory cytokines TNF- α , IL-1 β , and IL-8. Relative to the native protein, the secretion increased 1.2–2.0 fold for α -Syn, 1.2–8.8 fold for HSP60, and 2.1–16.7 fold for HMGB1 (Table S5). The mRNA expression of the investigated cytokines showed the same trend for modified HSP60 and HMGB1, but not for modified α -Syn (Fig. S2, Table S6). The mRNA results obtained for CXCL-10 indicate that the chemically modified proteins increased not only the activation of NF- κ B (MyD88 pathway), but also the activation of the IRF3 (TRIF/TRAF) pathway of TLR4 signaling [50,51]. The negative controls of native and peroxynitrite-modified OVA exhibited no substantial TLR4 and NF- κ B activity, cytokine secretion, or mRNA expression (Figs. 1–3, Fig. S2), and the applied protein concentrations did not affect the viability of the investigated cells (Figs. S3–S5), suggesting that the induced protein modifications were only relevant in the context of the TLR4-activating proteins. Pro-inflammatory cytokine responses via TLR4 are often heterogeneous at both the cell and population level [46–50], which provides an explanation for the variability of enhancement factors obtained from the cytokine expression and secretion experiments in this study (Tables S5 and S6). Nevertheless, the basic effects and overall trends observed for chemically modified vs. native DAMPs were consistent throughout our investigations - not only among replicate experiments but also with regard to the different experiments performed and different techniques applied in our study, which supports the main findings and conclusions as summarized and discussed below. Further investigations with larger replicate numbers and other cell types (primary cells) will be required for improved quantification of the cytokine effects and further mechanistic insights.

Overall, the available experimental results demonstrate that peroxynitrite treatment enhances the inflammatory potential of α -Syn,

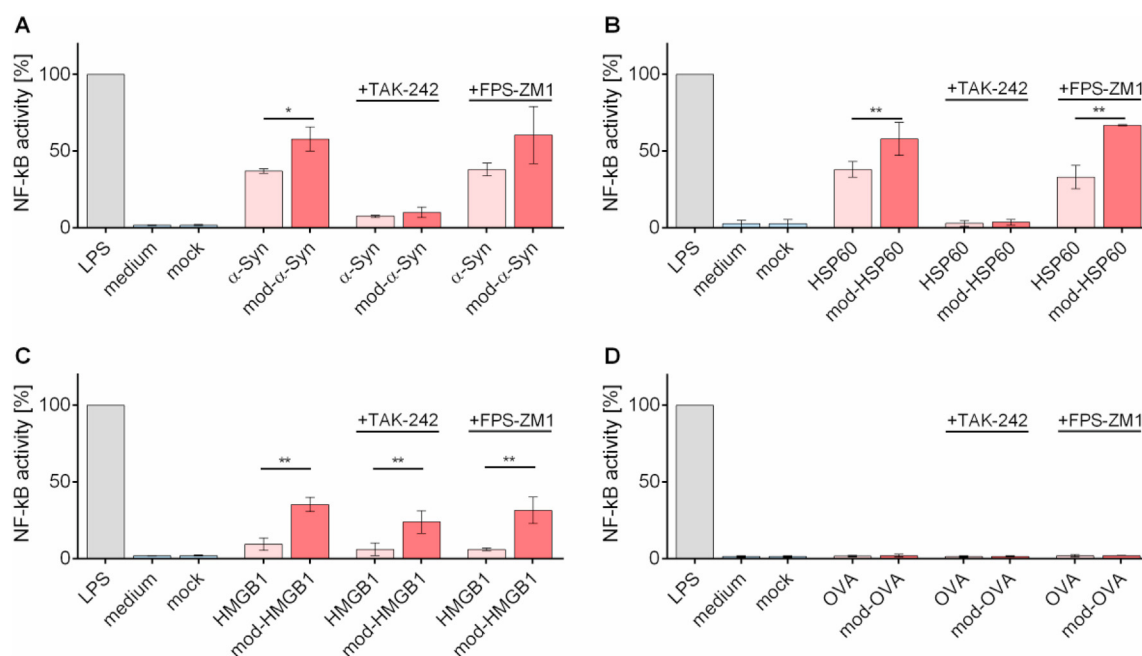


Fig. 2. NF- κ B activation by native and peroxynitrite-modified proteins. NF- κ B activity in THP-1-Lucia™ NF- κ B cells determined for α -Syn (A), HSP60 (B), HMGB1 (C), and OVA (D) normalized to LPS. Inhibition experiments with TLR4 antagonist TAK-242 and RAGE antagonist FPS-ZM1. Arithmetic mean values and standard deviations of three to four independent experiments performed in triplicates (* $p < 0.05$, ** $p < 0.01$).

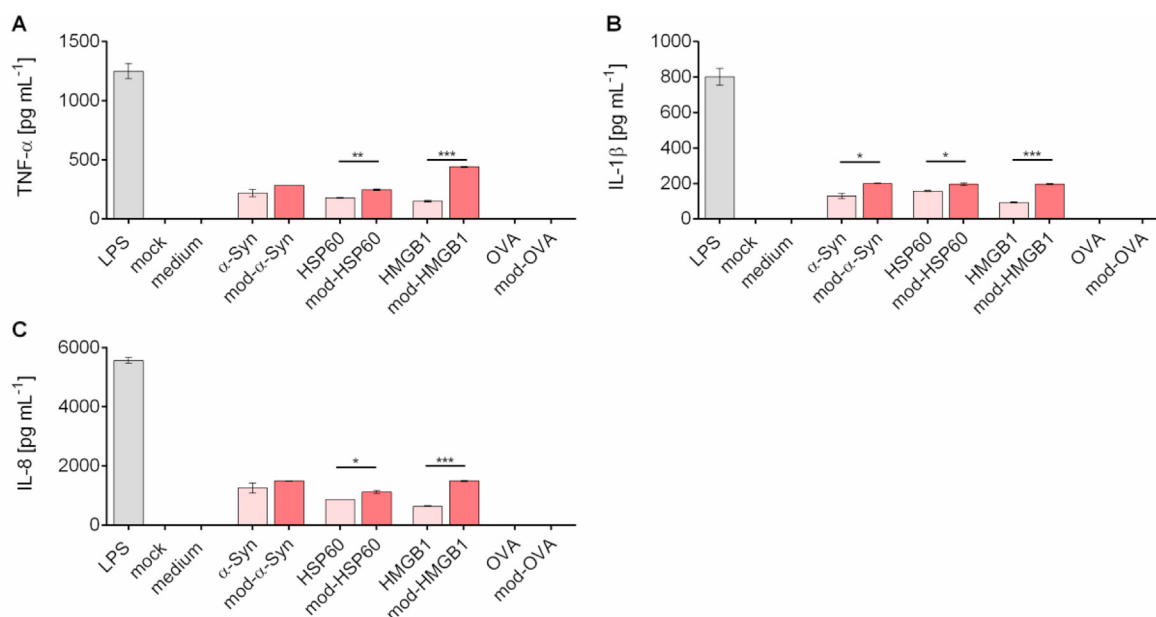


Fig. 3. Pro-inflammatory cytokine secretion in response to native and peroxynitrite-modified proteins. Release of TNF- α (A), IL-1 β (B), and IL-8 (C) determined for THP-1 monocytes after incubation over 24 h. Data for mock, medium, and OVA/mod-OVA are near or below the relevant limits of detection (\sim 2–20 pg mL⁻¹). Arithmetic mean values and standard deviations of a representative experiment performed in technical duplicates (*p < 0.05, **p < 0.01, ***p < 0.005).

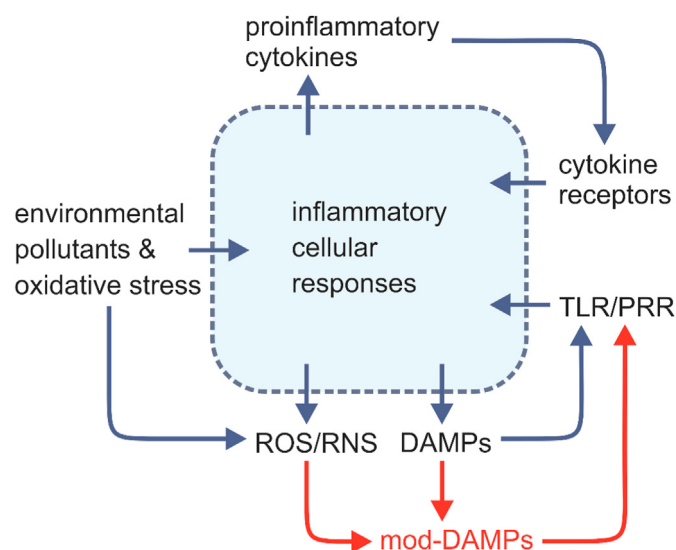


Fig. 4. Amplification of inflammatory processes and innate immune responses through chemically modified DAMPs. Environmental pollutants and oxidative stress can induce an increase of reactive oxygen and nitrogen species (ROS/RNS), the formation of chemically modified damage-associated molecular patterns (mod-DAMPs), an increase of pro-inflammatory signaling via Toll-like receptors and other pattern recognition receptors (TLR/PRR), an increase of pro-inflammatory cytokines, and further inflammatory cellular responses. Note that the results of this study and the schematic illustration are based on experiments with immortalized cell lines, and that further experiments with primary cells are required to confirm their applicability to the human immune system.

HSP60, and HMGB1 *in vitro*. This can be explained by changes in protein-receptor interactions related to chemical modifications like nitrotyrosine, intramolecular dityrosine crosslinks, protein dimers and higher oligomers as detected in the peroxynitrite-modified samples of the investigated proteins.

4. Discussion

Nitrotyrosine was detected in all chemically modified protein samples (Fig. S1, Table S2), and the introduction of a nitro group can strongly affect the chemical and physiological properties of a protein [52]. Notably, nitrotyrosine is more acidic than tyrosine, which can affect the isoelectric point of a protein, change the binding to receptors and ligands, and modulate downstream signaling cascades [7,12,13,53,54]. Nitration tends to enhance the immunogenicity of proteins, and nitrated proteins are thus used as model antigens or allergens [15,16,55–60]. The reason for this striking immunological property of nitrated proteins, which has also been linked to autoimmunity, is not completely clear [9,61]. The generation of neo-epitopes seems to be an important factor in adaptive immune responses [12,15], and nitrotyrosine was found to be associated with increased TLR4 signaling and innate immune responses related to chronic inflammatory diseases [8,52,62–64]. However, we here show for the first time that there is a direct enhancement of TLR4 activation by the peroxynitrite-induced modification of natural (human) DAMPs that play a role as innate immune activators in acute and chronic inflammation.

Besides nitrotyrosine, also dityrosine was detected in all chemically modified protein samples (Fig. S1). The detection of dityrosine in the monomeric form of the modified proteins implies that intramolecular crosslinks were formed and may have induced conformational changes affecting protein-receptor interactions. For HMGB1, it is well known that TLR4 binding depends on the oxidation state of the protein, and that an intramolecular disulfide bridge is crucial for TLR4 dimerization and activation [65,66]. By analogy, intramolecular dityrosine crosslinks among the tyrosine residues in HMGB1 might also induce or stabilize conformational arrangements that are relevant for protein-receptor interactions and TLR4 activation. Further investigations will be required to clarify if and how intramolecular dityrosine crosslinks may contribute to the enhancement of TLR4 activity observed for peroxynitrite-modified HMGB1 and other proteins.

Protein dimers and higher oligomers were detected in all chemically modified protein samples (Fig. S1, Table S2). They comprise more than

one receptor interaction domain, can act as multivalent ligands, and may thus more efficiently promote TLR4 dimerization and signaling [8,67–69]. Such multivalency effects are common in biological systems, where higher functional affinities are observed for dimeric and oligomeric agonists, leading to enhanced receptor clustering and signal transduction [70,71]. Thus, the formation of dimers and oligomers by intermolecular dityrosine crosslinking may well explain the enhanced TLR4 and NF- κ B activity observed upon stimulation with peroxynitrite-modified samples compared to the native form of the investigated proteins. For α -Syn, this is consistent with earlier studies reporting that oligomeric α -Syn can enhance TLR4 signaling and pro-inflammatory cytokine production in microglia and astrocytes, which may contribute to development and progression of Parkinson's disease [32,72]. Similar effects have been reported for the interaction of amyloid beta in Alzheimer's disease, where aggregates trigger TLR2 and TLR4 [73,74], and nitration critically enhances amyloid beta aggregation and plaque formation [75]. For all receptors within the TLR family [76,77] as well as RAGE [78,79] and other receptors [80,81], activation and signal transduction requires dimerization of the receptor molecules, which may be promoted by dimeric or oligomeric ligands. Thus, we suggest that the peroxynitrite-induced dimerization or oligomerization of HSP60 and HMGB1 may also play a critical role for PRR signaling in inflammatory diseases.

As outlined above, the proteins α -Syn, HSP60, and HMGB1 are involved in many severe diseases. If *in vivo* studies confirm that nitrotyrosine residues or dityrosine crosslinks in proteinous DAMPs play an important role in amplifying inflammatory processes through enhanced TLR4 signaling, the chemically modified proteins may serve as useful clinical markers providing mechanistic insights. Such markers and insight may also help to advance medical treatment options that involve scavenging of peroxynitrite [82–84] or the inhibition of peroxynitrite formation [85].

5. Conclusions

In this study, we have shown that peroxynitrite can induce chemical modifications that enhance the TLR4 activity and inflammatory potential of proteinous DAMPs like α -Syn, HSP60, and HMGB1.

Besides peroxynitrite, a wide range of other endogenous or exogenous ROS/RNS can also modify the chemical structure, properties, and effects of proteins [18]. In particular, air pollutants such as fine particulate matter, nitrogen oxides, and ozone can trigger or enhance oxidative stress, nitration and oligomerization of proteinous DAMPs and allergens, immune reactions, and feedback cycles of inflammation [1,8,27,55,56,86–88].

Fig. 4 illustrates how chemically modified DAMPs may amplify oxidative stress and innate immune responses through a positive feedback loop of pro-inflammatory signaling via TLR4 or other PRR. Such feedback and self-amplification provide a potential mechanistic rationale for the development of inflammatory disorders related to environmental pollution. In particular, it may help to explain the massive burden of disease attributable to air pollution, where the underlying chemical and physiological mechanisms are not yet well understood [4,89,90]. Environmental pollutants may generate exogenous ROS/RNS and oxidative stress, triggering inflammatory processes that lead to the formation of endogenous ROS/RNS and release of DAMPs. The DAMPs can activate PRR (TLR, RAGE, etc.) that induce further pro-inflammatory signaling and responses via transcription factors (NF- κ B, IRF3, etc.), cytokines and cytokine receptors (IL-1, IL-8, etc.). This positive feedback can be additionally enhanced if the DAMPs undergo chemical modification by ROS/RNS, and if the modified DAMPs lead to stronger activation of PRR than the native DAMPs, as observed in this study. Such effects may have important consequences for chronic neurodegenerative, cardiovascular or gastrointestinal diseases and allergies that are prevalent in modern societies. Note, however, that the experimental results of this study were obtained with immortalized cell

lines, and that primary cells should be used in follow-up studies to confirm the obtained data and conclusions with regard to the human immune system. We suggest and intend to pursue such follow-up studies further elucidating the underlying chemical and immunological interactions. Moreover, we suggest to consider and elucidate the role of environmental pollutants, and potential needs and perspectives for societal action with regard to the steeply increasing and globally pervasive human influence on air quality, climate, and public health in the Anthropocene [56,91].

Author contributions

KL and UP conceived and directed the study. KZ, ATK, KRS, ALL, and KL designed and performed the experiments. KZ, ATK, KRS, MGW, JFN, KL, and UP analyzed, interpreted and discussed the data. DW and DS contributed to the design, interpretation, and discussion. All authors contributed to the preparation and editing of the manuscript. KZ and ATK contributed equally.

Declaration of competing interest

The authors declare no conflict of interest.

Acknowledgement

This work was funded by the Max Planck Society and the Max Planck Graduate Center with the Johannes Gutenberg University Mainz. D. Schuppan receives project related support by research grants from the German Research Foundation DFG Schu 646/17–1 (ATI), DFG Pic/Sch SPP 1656 (Intestinal microbiota), DFG Schu 646/20–1 (Allergy), Collaborative Research Center 128 A08 (Multiple sclerosis), and from the Leibniz Foundation (WheatScan, SAW-2016-DFA-2). The authors acknowledge technical support by N. Bothen, C. S. Krevert, and N.-M. Kropf as well as helpful discussions with the members of the Mainz Program for Chemical Allergy (MPCA).

Appendix A. Supplementary data

Supplementary data to this article can be found online at <https://doi.org/10.1016/j.redox.2020.101581>.

References

- [1] M. Shiraiwa, K. Ueda, A. Pozzer, G. Lammel, C.J. Kampf, A. Fushimi, S. Enami, A.M. Arangio, J. Fröhlich-Nowoisky, Y. Fujitani, A. Furuyama, P.S.J. Lakey, J. Lelieveld, K. Lucas, Y. Morino, U. Pöschl, S. Takahama, A. Takami, H. Tong, B. Weber, A. Yoshino, K. Sato, Aerosol health effects from molecular to global scales, *Environ. Sci. Technol.* 51 (2017) 13545–13567, <https://doi.org/10.1021/acs.est.7b04417>.
- [2] T. Münzel, A. Daiber, Environmental stressors and their impact on health and disease with focus on oxidative stress, *Antioxidants Redox Signal.* 28 (2018) 735–740, <https://doi.org/10.1089/ars.2017.7488>.
- [3] F.J. Kelly, Oxidative stress: its role in air pollution and adverse health effects, *Occup. Environ. Med.* 60 (2003) 612–616, <https://doi.org/10.1136/oem.60.8.612>.
- [4] A.J. Cohen, M. Brauer, R. Burnett, H.R. Anderson, J. Frostad, K. Estep, K. Balakrishnan, B. Brunekreef, L. Dandona, R. Dandona, V. Feigin, G. Freedman, B. Hubbell, A. Jobling, H. Kan, L. Knibbs, Y. Liu, R. Martin, L. Morawska, C.A. Pope, H. Shin, K. Straif, G. Shaddick, M. Thomas, R. van Dingenen, A. van Donkelaar, T. Vos, C.J.L. Murray, M.H. Forouzanfar, Estimates and 25-year trends of the global burden of disease attributable to ambient air pollution: an analysis of data from the Global Burden of Diseases Study 2015, *Lancet* 389 (2017) 1907–1918, [https://doi.org/10.1016/S0140-6736\(17\)30505-6](https://doi.org/10.1016/S0140-6736(17)30505-6).
- [5] H. Sies, C. Berndt, D.P. Jones, Oxidative stress, *Annu. Rev. Biochem.* 86 (2017) 715–748, <https://doi.org/10.1146/annurev-biochem-061516-045037>.
- [6] A. van der Vliet, J.P. Eiserich, C.A. O'Neill, B. Halliwell, C.E. Cross, Tyrosine modification by reactive nitrogen species: a closer look, *Arch. Biochem. Biophys.* 319 (1995) 341–349, <https://doi.org/10.1006/abbi.1995.1303>.
- [7] K. Reinmuth-Selzle, C. Ackaert, C.J. Kampf, M. Samonig, M. Shiraiwa, S. Kofler, H. Yang, G. Gadermaier, H. Brandstetter, C.G. Huber, A. Duschl, G.J. Oostingh, Pöschl, nitration of the birch pollen allergen bet v 1.0101: efficiency and site-selectivity of liquid and gaseous nitrating agents, *J. Proteome Res.* 13 (2014) 1570–1577, <https://doi.org/10.1021/pr401078h>.

- [56] K. Reinmuth-Selzle, C.J. Kampf, K. Lucas, N. Lang-Yona, J. Fröhlich-Nowoisky, M. Shiraiwa, P.S.J. Lakey, S. Lai, F. Liu, A.T. Kunert, K. Ziegler, F. Shen, R. Sgarbanti, B. Weber, I. Bellinghausen, J. Saloga, M.G. Weller, A. Duschl, D. Schuppan, U. Pöschl, Air pollution and climate change effects on allergies in the Anthropocene: abundance, interaction, and modification of allergens and adjuvants, *Environ. Sci. Technol.* 51 (2017) 4119–4141, <https://doi.org/10.1021/acs.est.6b04908>.
- [57] A.C. Karle, G.J. Oostingh, S. Mutschlechner, F. Ferreira, P. Lackner, B. Bohle, G.F. Fischer, A.B. Vogt, A. Duschl, Nitration of the pollen allergen bet v 1.0101 enhances the presentation of bet v 1-derived peptides by HLA-DR on human dendritic cells, *PLoS One* 7 (2012) e31483, <https://doi.org/10.1371/journal.pone.0031483>.
- [58] L.L. Hardy, D.A. Wick, J.R. Webb, Conversion of tyrosine to the inflammation-associated analog 3'-nitrotyrosine at either TCR- or MHC-contact positions can profoundly affect recognition of the MHC class I-restricted epitope of lymphocytic choriomeningitis virus glycoprotein 33 by CD8 T Ce, *J. Immunol.* 180 (2008) 5956–5962, <https://doi.org/10.4049/jimmunol.180.9.5956>.
- [59] E. Untermayr, S.C. Diesner, G.J. Oostingh, K. Selzle, T. Pfaller, C. Schultz, Y. Zhang, D. Krishnamurthy, P. Starkl, R. Knittelfelder, E. Förster-Waldl, A. Pollak, O. Scheiner, U. Pöschl, E. Jensen-Jarolim, A. Duschl, Nitration of the egg-allergen ovalbumin enhances protein allergenicity but reduces the risk for oral sensitization in a murine model of food allergy, *PLoS One* 5 (2010) e14210, <https://doi.org/10.1371/journal.pone.0014210>.
- [60] A.S. Ondracek, D. Heiden, G.J. Oostingh, E. Fuerst, J. Fazekas-Singer, C. Bergmayr, J. Rohrhofer, E. Jensen-Jarolim, A. Duschl, E. Untermayr, Immune effects of the nitrated food allergen beta-lactoglobulin in an experimental food allergy model, *Nutrients* 11 (2019) 2463, <https://doi.org/10.3390/nu11102463>.
- [61] H.C. Birnboim, A.-M. Lemay, D.K.Y. Lam, R. Goldstein, J.R. Webb, Cutting edge: MHC class II-restricted peptides containing the inflammation-associated marker 3-nitrotyrosine evade central tolerance and elicit a robust cell-mediated immune response, *J. Immunol.* 171 (2003) 528–532, <https://doi.org/10.4049/jimmunol.171.2.528>.
- [62] S.A.B. Greenacre, H. Ischiropoulos, Tyrosine nitration: localisation, quantification, consequences for protein function and signal transduction, *Free Radic. Res.* 34 (2001) 541–581, <https://doi.org/10.1080/10715760100300471>.
- [63] J.M. Souza, G. Peluffo, R. Radi, Protein tyrosine nitration — functional alteration or just a biomarker? *Free Radic. Biol. Med.* 45 (2008) 357–366, <https://doi.org/10.1016/j.freeradbiomed.2008.04.010>.
- [64] X. Tun, K. Yasukawa, K. Yamada, Nitric oxide is involved in activation of toll-like receptor 4 signaling through tyrosine nitration of src homology protein tyrosine phosphatase 2 in murine dextran sulfate-induced colitis, *Biol. Pharm. Bull.* 41 (2018) 1843–1852, <https://doi.org/10.1248/bpb.b18-00558>.
- [65] C. Janko, M. Filipović, L.E. Munoz, C. Schorn, G. Schett, I. Ivanović-Burmazović, M. Herrmann, Redox modulation of HMGB1-related signaling, *Antioxidants Redox Signal.* 20 (2014) 1075–1085, <https://doi.org/10.1089/ars.2013.5179>.
- [66] S. Sun, M. He, S. VanPatten, Y. Al-Abed, Mechanistic insights into high mobility group box-1 (HMGB1)-induced Toll-like receptor 4 (TLR4) dimer formation, *J. Biomol. Struct. Dyn.* 37 (2019) 3721–3730, <https://doi.org/10.1080/07391102.2018.1526712>.
- [67] C.L. Krüger, M.-T. Zeuner, G.S. Cottrell, D. Widera, M. Heilemann, Quantitative single-molecule imaging of TLR4 reveals ligand-specific receptor dimerization, *Sci. Signal.* 10 (2017), <https://doi.org/10.1126/scisignal.aan1308> ean1308.
- [68] S.L. Latty, J. Sakai, L. Hopkins, B. Verstak, T. Paramo, N.A. Berglund, E. Cammarota, P. Cicuta, N.J. Gay, P.J. Bond, D. Klenerman, C.E. Bryant, Activation of Toll-like receptors nucleates assembly of the MyDDosome signaling hub, *Elife* 7 (2018) 1–15, <https://doi.org/10.7554/eLife.31377>.
- [69] J. Neumann, K. Ziegler, M. Gelléri, J. Fröhlich-Nowoisky, F. Liu, I. Bellinghausen, D. Schuppan, U. Birk, U. Pöschl, C. Cremer, K. Lucas, Nanoscale distribution of TLR4 on primary human macrophages stimulated with LPS and ATI, *Nanoscale* 11 (2019) 9769–9779, <https://doi.org/10.1039/C9NR00943D>.
- [70] K.W. Foreman, A general model for predicting the binding affinity of reversibly and irreversibly dimerized ligands, *PLoS One* 12 (2017) e0188134, <https://doi.org/10.1371/journal.pone.0188134>.
- [71] L.L. Kiessling, J.E. Gestwicki, L.E. Strong, Synthetic multivalent ligands as probes of signal transduction, *Angew. Chem. Int. Ed.* 45 (2006) 2348–2368, <https://doi.org/10.1002/anie.200502794>.
- [72] L. Fellner, R. Irschick, K. Schanda, M. Reindl, L. Klimaschewski, W. Poewe, G.K. Wenning, N. Stefanova, Toll-like receptor 4 is required for α -synuclein dependent activation of microglia and astroglia, *Glia* 61 (2013) 349–360, <https://doi.org/10.1002/glia.22437>.
- [73] M. Jana, C.A. Palencia, K. Pahan, Fibrillar amyloid- β peptides activate microglia via TLR2: implications for Alzheimer's disease, *J. Immunol.* 181 (2008) 7254–7262, <https://doi.org/10.4049/jimmunol.181.10.7254>.
- [74] M.L.D. Udan, D. Ajit, N.R. Crouse, M.R. Nichols, Toll-like receptors 2 and 4 mediate A β (1–42) activation of the innate immune response in a human monocytic cell line, *J. Neurochem.* 104 (2008) 524–533, <https://doi.org/10.1111/j.1471-4159.2007.05001.x>.
- [75] M.P. Kummer, M. Hermes, A. Delekarte, T. Hammerschmidt, S. Kumar, D. Terwel, J. Walter, H.-C. Pape, S. König, S. Roeber, F. Jessen, T. Klockgether, M. Korte, M.T. Heneka, Nitration of tyrosine 10 critically enhances amyloid β aggregation and plaque formation, *Neuron* 71 (2011) 833–844, <https://doi.org/10.1016/j.neuron.2011.07.001>.
- [76] B. Beutler, Inferences, questions and possibilities in Toll-like receptor signalling, *Nature* 430 (2004) 257–263, <https://doi.org/10.1038/nature02761>.
- [77] J.Y. Kang, J.-O. Lee, Structural biology of the toll-like receptor family, *Annu. Rev. Biochem.* 80 (2011) 917–941, <https://doi.org/10.1146/annurev-biochem-052909-141507>.
- [78] J. Xue, M. Manigrasso, M. Scalabrini, V. Rai, S. Reverdatto, D.S. Burz, D. Fabris, A.M. Schmidt, A. Shekhtman, Change in the molecular dimension of a RAGE-ligand complex triggers RAGE signaling, *Structure* 24 (2016) 1509–1522, <https://doi.org/10.1016/j.str.2016.06.021>.
- [79] H. Zong, A. Madden, M. Ward, M.H. Mooney, C.T. Elliott, A.W. Stitt, Homodimerization is essential for the receptor for advanced glycation end products (RAGE)-mediated signal transduction, *J. Biol. Chem.* 285 (2010) 23137–23146, <https://doi.org/10.1074/jbc.M110.133827>.
- [80] M.R. Walter, The molecular basis of IL-10 function: from receptor structure to the onset of signaling, in: S. Fillatreau, A. O'Garra (Eds.), *Curr. Top. Microbiol. Immunol.* Springer, Berlin, Heidelberg, 2014, pp. 191–212, https://doi.org/10.1007/978-3-662-43492-5_9.
- [81] M. Simons, E. Gordon, L. Claesson-Welsh, Mechanisms and regulation of endothelial VEGF receptor signalling, *Nat. Rev. Mol. Cell Biol.* 17 (2016) 611–625, <https://doi.org/10.1038/nrm.2016.87>.
- [82] A. Daiber, S. Daub, M. Bachschmid, S. Schildknecht, M. Oelze, S. Steven, P. Schmidt, A. Megner, M. Wada, T. Tanabe, T. Münzel, S. Bottari, V. Ullrich, Protein tyrosine nitration and thiol oxidation by peroxynitrite—strategies to prevent these oxidative modifications, *Int. J. Mol. Sci.* 14 (2013) 7542–7570, <https://doi.org/10.3390/ijms14047542>.
- [83] P. Pacher, J. Beckman, L. Liaudet, Nitric oxide and peroxynitrite, *Physiol. Rev.* 87 (2007) 315–424, <https://doi.org/10.1152/physrev.00029.2006>.
- [84] S. Das, F. Alhasson, D. Dattaroy, S. Pourhoseini, R.K. Seth, M. Nagarkatti, P.S. Nagarkatti, G.A. Michelotti, A.M. Diehl, B. Kalyanaraman, S. Chatterjee, NADPH oxidase-derived peroxynitrite drives inflammation in mice and human nonalcoholic steatohepatitis via TLR4-lipid raft recruitment, *Am. J. Pathol.* 185 (2015) 1944–1957, <https://doi.org/10.1016/j.ajpath.2015.03.024>.
- [85] T.L. Poulos, H. Li, Nitric oxide synthase and structure-based inhibitor design, *Nitric Oxide* 63 (2017) 68–77, <https://doi.org/10.1016/j.niox.2016.11.004>.
- [86] C.J. Kampf, F. Liu, K. Reinmuth-Selzle, T. Berkemeier, H. Meusel, M. Shiraiwa, U. Pöschl, Protein cross-linking and oligomerization through dityrosine formation upon exposure to ozone, *Environ. Sci. Technol.* 49 (2015) 10859–10866, <https://doi.org/10.1021/acs.est.5b02902>.
- [87] P.S.J. Lakey, T. Berkemeier, H. Tong, A.M. Arangio, K. Lucas, U. Pöschl, M. Shiraiwa, Chemical exposure-response relationship between air pollutants and reactive oxygen species in the human respiratory tract, *Sci. Rep.* 6 (2016), <https://doi.org/10.1038/srep32916> 32916.
- [88] M. Shiraiwa, K. Selzle, U. Pöschl, Hazardous components and health effects of atmospheric aerosol particles: reactive oxygen species, soot, polycyclic aromatic compounds and allergenic proteins, *Free Radic. Res.* (2012) 1–13, <https://doi.org/10.3109/10715762.2012.663084>.
- [89] J. Lelieveld, K. Klingmüller, A. Pozzer, U. Pöschl, M. Fnais, A. Daiber, T. Münzel, Cardiovascular disease burden from ambient air pollution in Europe reassessed using novel hazard ratio functions, *Eur. Heart J.* 40 (2019) 1590–1596, <https://doi.org/10.1093/eurheartj/ehz135>.
- [90] J. Lelieveld, U. Pöschl, Chemists can help to solve the air-pollution health crisis, *Nature* 551 (2017) 291–293, <https://doi.org/10.1038/d41586-017-05906-9>.
- [91] U. Pöschl, M. Shiraiwa, Multiphase chemistry at the atmosphere–biosphere interface influencing climate and public health in the Anthropocene, *Chem. Rev.* 115 (2015) 4440–4475, <https://doi.org/10.1021/cr500487s>.